RSC Advances

This is an *Accepted Manuscript*, which has been through the Royal Society of Chemistry peer review process and has been accepted for publication.

Accepted Manuscripts are published online shortly after acceptance, before technical editing, formatting and proof reading. Using this free service, authors can make their results available to the community, in citable form, before we publish the edited article. This *Accepted Manuscript* will be replaced by the edited, formatted and paginated article as soon as this is available.

You can find more information about *Accepted Manuscripts* in the **Information for Authors**.

ROYAL SOCIETY OF CHEMISTRY

www.rsc.org/advances

RSC ADVANCES

ARTICLE

Anchoring of Pd(II) complex in functionalized MCM-41 as an efficient and recoverable novel nano catalyst in C-C, C-O and C-N coupling reactions using Ph$_3$SnCl

Arash Ghorbani-Choghamarani[a*], Farzad Nikpour[b], Farshid Ghorbani[c], Forugh Havasi[b]

Anchored palladium (II) in functionalized MCM-41 mesoporous silica was prepared and used as an efficient, recoverable and thermally stable heterogeneous nano catalyst for C-C, C-O and C-N bond formation in cross-coupling reactions in the presence of Ph$_3$SnCl. MCM-41 was prepared trough hydrothermal synthesis using tetraethyl orthosilicate (Si(OC$_2$H$_5$)$_4$) as silica source and cetyltrimethylammonium bromide (CTAB) as a template. The structure of functionalized MCM-41 was studied by FT-IR, XRD, SEM, TEM, TGA, EDS, ICP and BET techniques.

1 Introduction

Since the discovery of ordered mesoporous silica materials [1, 2], different synthetic routes have been reported for their preparation using cationic surfactants as a template [3-5]. Generally, the preparation process consists of the formation of micelles in aqueous solution followed by the polymerization of an inorganic source and the removal of surfactants from the pores [5]. MCM-41 has a hexagonal arrangement of one-dimensional mesopores with diameters ranging from 2 to 10 nm [2]. Due to its unique properties such as high surface area, homogeneity of the pores, good thermal stability, tunable and accessible pores, MCM-41 has been a focus for several research areas like nanoscience [6], catalysis [7 and 8], environmental purification [9], adsorption [10] and drug delivery [11]. The nature of MCM-41 pore structure can be used to functionalize via reaction with alkoxysilyl compounds and then incorporation of metal complexes into the channel walls [12]. Stepnicka [13, 14] and Karimi [15] modified mesoporous silica with various *N*-groups and loaded this support with palladium; The resulting material was applied as a catalyst for organic synthesis. C-C and C-Heteroatom coupling reactions catalyzed by transition-metals are among the most important reactions in organic synthesis [16-19]. Palladium has been the most used transition metal catalyst for the various coupling reactions [20, 21]. In general, the activity of homogeneous palladium catalysts such as Pd(OAc)$_2$ and PdCl$_2$ is sufficiently high, However, they suffer from the drawbacks of difficult separation and recovering

from the reaction mixture as well as serious environmental pollution which have limited their applications. Development of heterogeneous palladium catalysts to overcome the above drawbacks has important theoretical and practical significance and also is one of the main objectives of green chemistry. Thus, solid materials such as polymer materials, carbon, zeolite and different types of silica (amorphous silica, mesoporous molecular sieves, solids obtained by co-condensation of silicate precursors and many others) have been used to immobilize the palladium catalysts [22-25].

In this paper, we report the synthesis and characterization of Pd(II) complex supported on dithizone-functionalized nanostructured MCM-41 (MCM-41-dtz-Pd(II)) as novel and efficient catalyst for the C-C, C-O and C-N bond formation in coupling reactions in the presence of triphenyltin chloride under mild reaction conditions.

2 Results and discussion

In continuation of our recent success in the introduction of new catalysts [7, 26], Herein we report the synthesis of Pd(II) complex supported on dithizone-functionalized nanostructured MCM-41 (MCM-41-dtz-Pd(II)) as novel and efficient catalyst for the C-C, C-O and C-N bond formation in coupling reactions in the presence of triphenyltin chloride under mild reaction conditions (Scheme 1).

Address correspondence to A. Ghorbani-Choghamarani, Department of Chemistry, Faculty of Science, Ilam University, P.O. Box 69315516, Ilam, Iran; Tel/Fax: +98 841 2227022; E-mail address:arashghch58@yahoo.com or a.ghorbani@mail.ilam.ac.ir
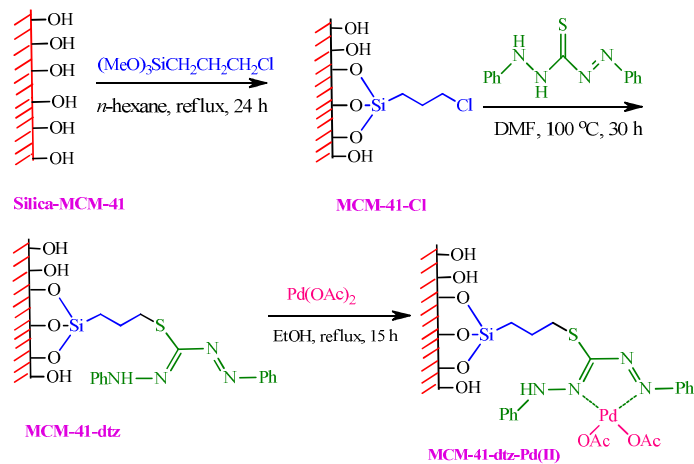
Scheme1. Synthesis of MCM-41-dtz-Pd(II)

Figure 1. FT-IR spectra of (a) MCM-41 (b) MCM-41-*n*Pr-Cl, (c) MCM-41-dtz, (d) MCM-41-dtz-Pd(II) and (e) recovered MCM-41-dtz-Pd(II)

2.1 Catalyst characterization

The synthesis of the MCM-41-dtz-Pd(II) schematically shown in Scheme 1. FT-IR spectra were recorded separately at different stages of the preparation (Fig. 1). Curve **a** in Fig. 1 is the spectrum of the MCM-41 and curve **b** is the spectrum of the MCM-41-*n*Pr-Cl. The absorption band presented at 962 cm^{-1} is attributable to Si–O vibrations [27]. Absorption bands at 1235, 1080, 799 and 461 cm^{-1} are assignable to the asymmetric and symmetric stretching vibrations of the mesoporous framework (Si–O–Si). The O-H stretching vibration bands appeared at 3478 cm^{-1}. The presence of the anchored CPTMS group is confirmed by C–H stretching vibrations at 2959 and 2853 cm^{-1} in MCM-41-*n*Pr-Cl spectra. The curve **c** shows stretching vibrations at 1640 cm^{-1} (C=N), 1430 cm^{-1} (C=C) and broad band at about 3447 cm^{-1} (O-H and N–H) for MCM-41-dtz. Curve **d** shows the FT-IR spectrum after adsorption of Pd(II) onto MCM-41-dtz and the curve e, which is the spectrum of the recovered MCM-41-dtz-Pd(II), shows that the catalyst is stable during the coupling reactions.
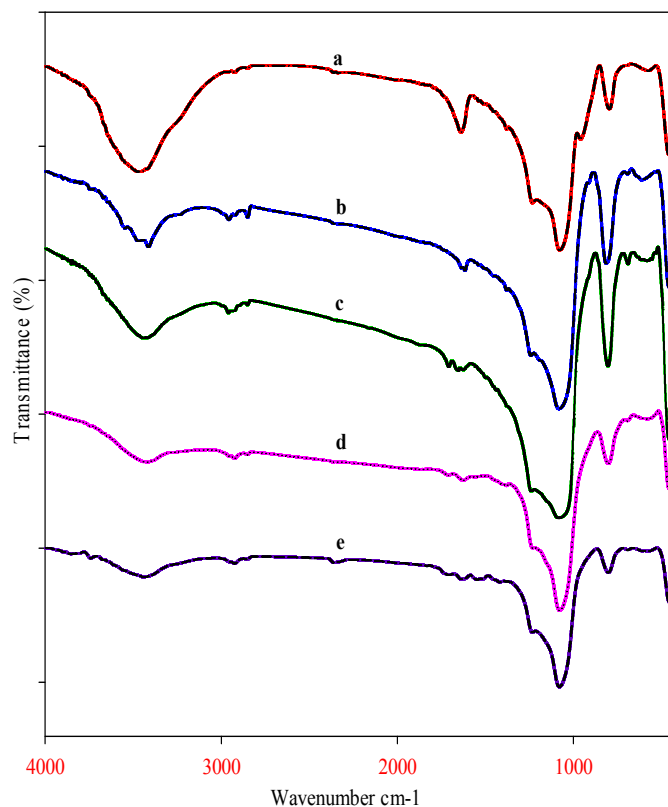
The small angle powder X-ray diffraction patterns for MCM-41, MCM-41-*n*Pr-Cl, MCM-41-dtz and MCM-41-dtz-Pd(II) are shown in Fig. 2. The pattern of the MCM-41 shows the presence of the three reflection peaks corresponding to 100, 110 and 200, typically, confirming the presence of ordered hexagonal mesoporous structure of MCM-41 [28]. The values of d-spacing (100) for XRD pattern of MCM-41, MCM-41-*n*Pr-Cl, MCM-41-dtz and MCM-41-dtz-Pd(II) were 39.38, 35.82, 35.07 and 35.43 A° , respectively. A unit cell parameter, a_0 was obtained using the following equation:

$$a_0 = \frac{2d_{100}}{\sqrt{3}}$$

All the samples showed one intense peak (100) and the patterns were similar to that of pure silica MCM-41, indicating that the functionalized MCM-41 materials contain ordered hexagonal arrays of one-dimensional channel structure. However, the peak intensity decreased and the higher order (110 and 200) diffractions became less resolved and disappeared at last, showing that the mesopore ordering decreased as more substance were anchored on the surface of MCM-41. The XRD patterns were essentially the same as that of the calcined MCM-41, signifying the conservation of the mesoporous texture during the post grafting process. These changes might be due to a partial loss of the space correlation of the pores were commonly observed in studies of silylation of mesoporous silica. The intensity of the Bragg-reflections originates from the difference in the scattering power between the silica walls and the empty pores. Due to the presence of the complex inside the pores, the amount of scattering power within the pores is increased, resulting in overall loss of intensity due to phase cancellation

between pore walls and the guest complex [29]. Therefore, it can be concluded that the formation of the catalyst has taken place preferentially inside the pore system of the MCM-41.
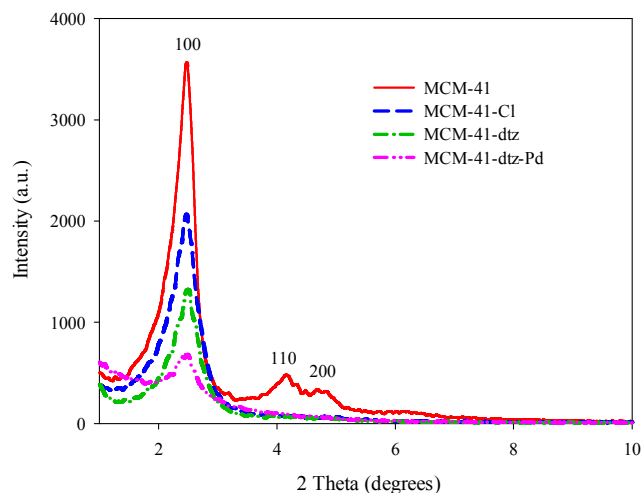

Figure 2. Low angle XRD patterns of MCM-41, MCM-41-*n*Pr-Cl, MCM-41-dtz and MCM-41-dtz-Pd(II).

The thermogravimetric analysis (TGA) curves of MCM-41, MCM-41-*n*Pr-Cl, MCM-41-dtz and MCM-41-dtz-Pd(II) show the mass loss of the organic materials as they decompose upon heating (Fig. 3). According to these curves, two weight loss steps were observed. The first mass loss occurs at a temperature range of 25-300 $^{\circ}$C that is related to the loss of physically and chemically adsorbed water and organic solvents. The second mass loss occurs at a temperature range of 300-780 $^{\circ}$C, which is related to the thermal decomposition of organochloropropyl fragments and organic ligands in the complex.
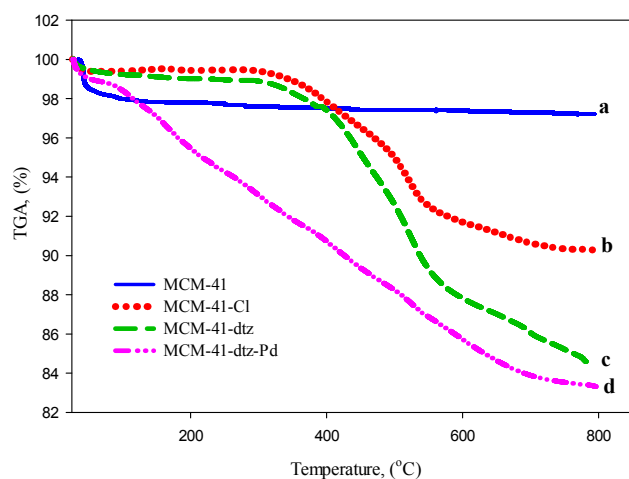

Figure 3. TGA curves of MCM-41 (a), MCM-41-*n*Pr-Cl (b), MCM-41-dtz (c) and MCM-41-dtz-Pd(II) (d).

The metal content of MCM-41-dtz-Pd(II) was investigated using EDS. A typical EDS spectrum taken from the MCM-41-dtz-Pd(II) was shown in Fig. 4**a**, where peaks associated with Si, C, O, N, S and Pd can be distinguished.The EDS spectra at different points of the image (Fig. 4**a**) confirm the presence of Pd in the mesoporous silica matrix. The amount of Pd incorporated into the

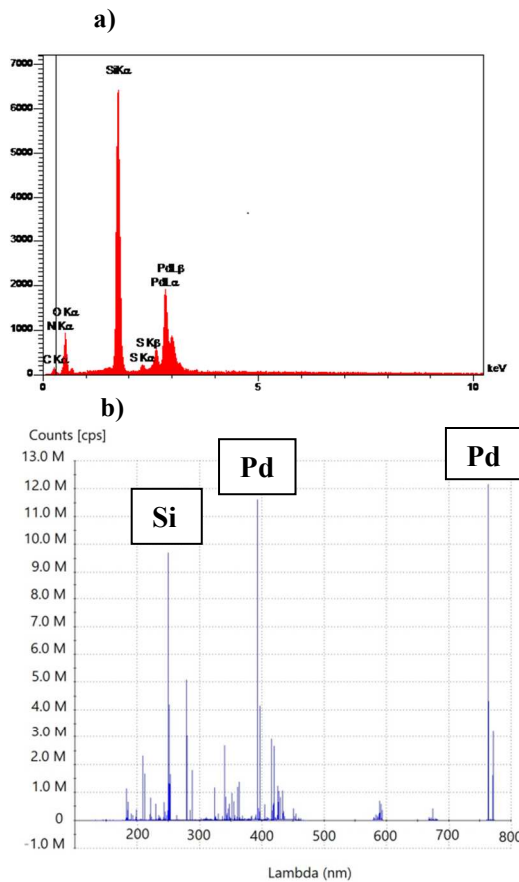mesoporoussilicafound 13.88%, determined byinductively coupled plasma optical emission spectrometry (ICP-OES) (Fig. 4**b**).

Figure 4.(**a**) EDS pattern of MCM-41-dtz-Pd(II); (**b**) ICP-OES pattern of MCM-41-dtz-Pd(II).

In order to determine the textural properties, the nitrogen adsorption–desorption isotherms were measured using a BEL sorp-mini II volumetric adsorption analyzer in order to determine the textural properties. All of the samples were degassed at 100°C under an argon gas flow for 3 h before analysis.

The N_2 adsorption and desorption isotherms of MCM-41, MCM-41-dtz-Pd(II) are shown in Fig. 5 indicating the functionalized MCM-41 have narrower pore diameter and lower absorption volume which are identical with the result obtained by XRD. The information derived from the isotherms is in agreement with the XRD patterns (Fig. 2). The BET (Brunauer–Emmett–Teller) surface area and the pore diameter were also determined for MCM-41 and MCM-41-dtz-Pd(II). BET analysis of MCM-41 shows a surface area of 986 m^2/g and a pore volume of 0.71cm^3/g. Functionalization of CPTMS with Pd(II) complex lead to a decrease in the surface area (507 m^2/g.) and pore volume (0.26 cm^3/g). The specific pore volume, BET surface area and average BJH (Barrett-Joyner-Halenda) pore diameter of functionalized MCM-41 decreased with increasing substance anchored on the surface of MCM-41, as shown in Table 1. The wall thickness of MCM-41and MCM-41-dtz-Pd(II) where calculated by the following equation:

$$\text{wall tickness} = \frac{2d_{1\,0\,0}}{\sqrt{3}} - D_{BJH}$$

These results are attributed to the occupation of large organic molecules on the inner surface of the pores. Although the ordering of MCM-41-dtz-Pd(II) decreased, they still have high surface area.

Table 1. Textural parameters deduced from nitrogen sorption isotherms

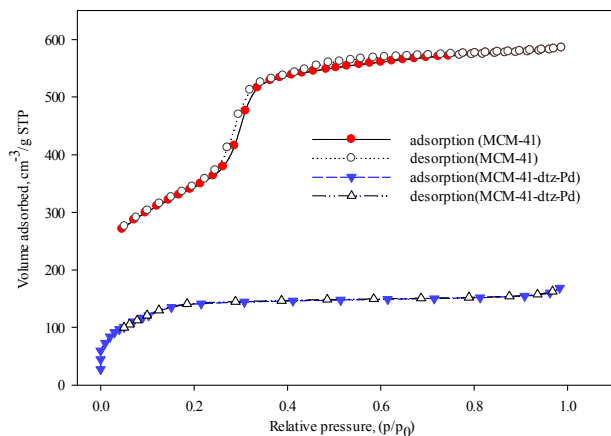| Sample	S_{BET} (m^2/g)	Pore diameter by BJH method (nm)	Pore volume (cm^3/g)	Wall diameter (nm)
MCM-41	986	3.6	0.71	0.9
MCM-41-dtz-Pd(II)	507	1.2	0.26	2.9

Figure 5. Nitrogen adsorption/desorption isotherms MCM-41, MCM-41-dtz-Pd(II).

Morphological changes were investigated by scanning electron microscopy (SEM) of MCM-41 and MCM-41-dtz-Pd(II) (Fig. 6**a**, 6**b**). Fig. 6**c** and Fig. 6**d** show transmission electron micrographs of representative regions of MCM-41. Highly ordered long-range hexagonal arrangement of the pores can be clearly observed. The TEM results are in good agreement with the XRD.

(a)

(b)

(c)

(d)
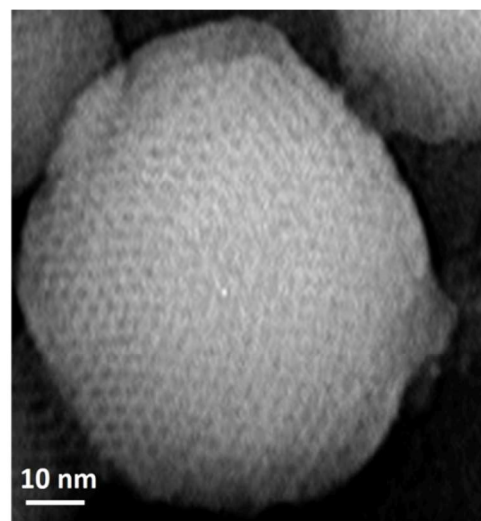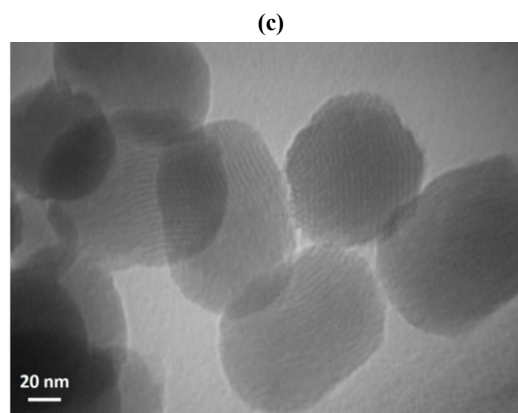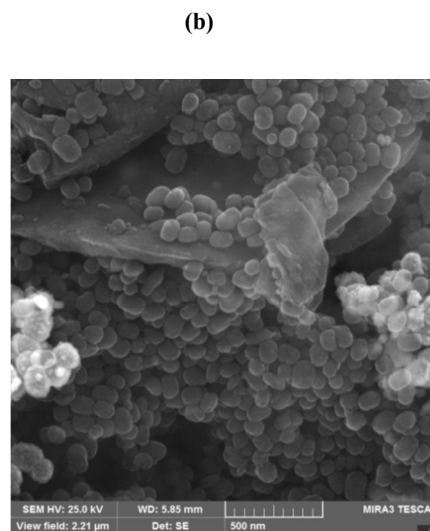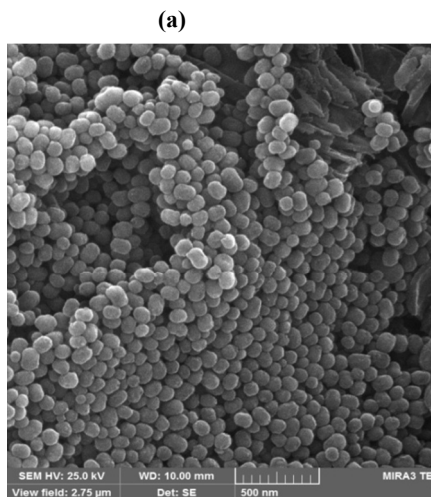

Figure 6. SEM image of calcined MCM-41/ MCM-41-dtz-Pd (**a** and **b**), TEM image of calcined MCM-41(**c** and **d**).

2.2 Catalytic studies

After preparation and characterization of MCM-41-dtz-Pd, its catalytic activities were investigated in some of the coupling reactions such as C-C and C-heteroatom bond formation by triphenyltin chloride (as a phenylating agent). Initially, we

examined the reaction of phenol with Ph_3SnCl in different solvents, bases and various amounts of MCM-41-dtz-Pd(II) (Table 2). Applying 5 mg of MCM-41-dtz-Pd(II) and 10 eq. of Et_3N as base and solvent at room temperature, is the best conditions for cross-coupling of Ph_3SnCl (0.5 mmol) with phenol (1 mmol) (Table 2, entry 9). Other bases such as K_2CO_3 and nPr_3N and different solvents including CH_2Cl_2, PEG, EtOAc and THF were tested and the obtained results were unsatisfactory.
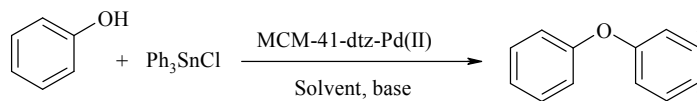

Table 2. Optimization of different parameters for the reaction of phenol with Ph_3SnCl^a

Entry	Cat. (mg)	Solvent	Base (eq.)	Temp (°C)	Time (h)	Yield (%)[b]
1	0	-	Et_3N (10)	rt	72	0
2	0	PEG	Et_3N (10)	80	72	0
3	4	PEG	Et_3N (5)	80	29	75
4	5	PEG	Et_3N (5)	80	27	84
5	5	PEG	Et_3N (5)	rt	30	88
6	7	PEG	Et_3N (5)	80	27	80
7	10	PEG	Et_3N (5)	80	28	78
8	4	-	Et_3N (10)	rt	26	85
9	5	-	Et_3N (10)	rt	24	95
10	7	-	Et_3N (10)	rt	24	90
11	10	CH_2Cl_2	Et_3N (5)	rt	36	72
12	10	EtOAc	Et_3N (5)	60	34	60
13	5	PEG	K_2CO_3 (2)	80	26	70
14	5	-	nPr_3N (10)	rt	35	65
15	5	THF	Et_3N (5)	50	40	50

[a]Reaction conditions: phenol (1 mmol), Ph_3SnCl (0.5 mmol).
[b]Isolated Yield.

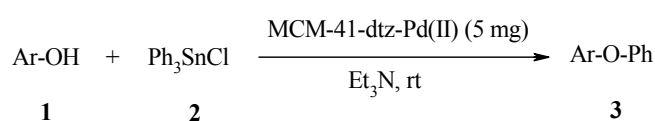Results of coupling reaction of various phenols with Ph_3SnCl have been summarized in Table 3.

Table 3. The reaction of phenol derivatives with Ph_3SnCl at room temperature

Entry	Ar	Time (h)	Yield 3 (%)[a,b]	Mp (°C) [Ref.]
1	Ph	24	95	yellowish oil [30]
2	4-MePh	22	92	yellowish oil [31]
3	3-MePh	25	89	yellowish oil [32]
4	4-MeOPh	23	94	yellowish oil [32]
5	3-MeOPh	25	90	yellowish oil [33]
6	4-BrPh	20	92	yellowish oil [33]

7	3-BrPh	22	85	yellowish oil [17]
8	4-ClPh	21	85	yellowish oil [33]
9	4-NO_2Ph	18	90	54-56 [17]
10	1-Naph	27	85	colorless oil [33]
11	2-Naph	24	87	46-48 [33]

[a] All the products were identified and characterized by comparison of their physical and spectral data with those of authentic samples. [b] Isolated Yield.

Optimizing the cross-coupling reaction conditions of aniline (1 mmol) with Ph_3SnCl (0.5 mmol) as a model reaction showed the effective mixture of MCM-41-dtz-Pd(II) (5 mg) and Et_3N (10 eq., 1.4 mL) as base and solvent at room temperature (Table 4, entry 4). Table 5 shows the reaction of Ph_3SnCl with a variety of amines. The results indicate that aliphatic amines (entries 9-13) and heterocyclic amines (entries 7 and 8) produce the coupled product in good yields. Steric effect is also observed in the case of 2-methylaniline which proceeds in relatively lower yield (entry 3). In addition to amines, the reaction of benzamide as a model reaction for amides is performed successfully (entry 14).
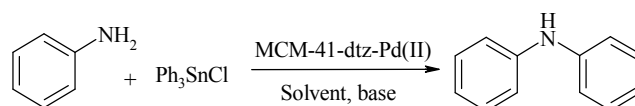
Table 4. Optimization of different parameters for the reaction of aniline with Ph_3SnCl^a

Entry	Cat. (mg)	Solvent	Base (eq.)	Temp (°C)	Time (h)	Yield (%)[b]
1	0	-	Et_3N(10)	rt	40	0
2	0	PEG	Et_3N(10)	80	40	0
3	4	-	Et_3N (10)	rt	16	87
4	5	-	Et_3N (10)	rt	15	95
5	7	-	Et_3N (10)	rt	16	91
6	5	-	Et_3N (10)	80	13	80
7	5	PEG	Et_3N (5)	80	17	80
8	5	EtOAc	Et_3N (5)	60	22	70
9	5	CH_2Cl_2	Et_3N (5)	rt	25	60

[a]Reaction conditions: 1mmol of aniline, 0.5 mmol of Ph_3SnCl
[b]Isolated Yield.
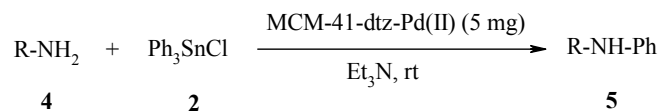
Table 5. The reaction of amines with Ph_3SnCl at room temperature

Entry	Amine 4	Time (h)	Yield 5 (%)[a,b]	Mp (°C) [Ref.]
1		15	95	54-55 [34]
2		15	90	88 [35]

3	2-methylaniline (Me, NH2)	18	70	38 [34]
4	4-Cl aniline (NH2)	14	88	73-74 [36]
5	4-Br aniline (NH2)	13	92	87-89 [34]
6	4-NO2 aniline (O_2N, NH2)	10	94	134-136 [35]
7	pyrrole (NH)	16	87	60-62 [34]
8	indole (N-H)	16	85	colorless oil [34]
9	benzylamine (NH2)	27	93	35-37 [34]
10	propylamine (NH2)	16	80	colorless oil [17]
11	butylamine (NH2)	16	78	colorless oil [37]
12	dibutylamine (NH)	17	78	colorless oil [34]
13	morpholine (HN O)	16	82	55 [34]
14	benzamide (NH2, O)	15	88	163-165 [37]

[a] All the products were identified and characterized by comparison of their physical and spectral data with those of authentic samples. [b] Isolated Yield.

Results of Table 3 (entries 6-8) and Table 5 (entries 4, 5) show the chemoselectivity of the reactions, in which, C-heteroatom bond formation is preferred to C-C bond formation. The reactivity of MCM-41-dtz-Pd(II) as catalyst was also examined in the Stille cross-coupling reaction of aryl halides with Ph_3SnCl. The preliminary investigation was to screen the solvent, base and different amounts of catalyst on the reaction of iodobenzene with Ph_3SnCl (Table 6).
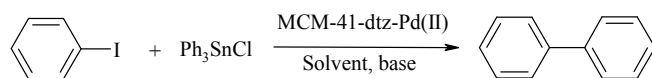
$$\text{PhI} \quad + \quad Ph_3SnCl \xrightarrow[\text{Solvent, base}]{\text{MCM-41-dtz-Pd(II)}} \text{Ph-Ph}$$

Table 6. Coupling of iodobenzene with Ph_3SnCl catalyzed by MCM-41-dtz-Pd(II) in the presence of different solvents and bases[a]

Entry	Ph_3SnCl (mmol)	Cat. (mg)	Solvent	Base	Temp (^{o}C)	Time (h)	Yield (%)[b]
1	0.5	0	PEG	K_2CO_3	80	24	0
2	0.5	4	PEG	K_2CO_3	rt	5	87
3	0.5	5	PEG	K_2CO_3	rt	3	97
4	0.5	7	PEG	K_2CO_3	rt	3.5	90
5	0.5	5	PEG	Et_3N	rt	9	75
6	0.5	5	PEG	nPr_3N	rt	13	68
7	0.5	5	PEG	K_2CO_3	80	2.5	94
8	0.5	5	PEG	Et_3N	80	7	82
9	0.5	5	PEG	nPr_3N	80	9	72
10	0.5	5	EtOH	K_2CO_3	70	9	80
11	0.5	10	EtOH	K_2CO_3	70	9.5	81
12	0.5	5	EtOH	Et_3N	70	11	60
13	0.5	5	EtOAc	K_2CO_3	60	10	80
14	0.5	5	EtOAc	Et_3N	60	12	75
15	0.5	5	CH_2Cl_2	K_2CO_3	60	11	70
16	0.33	5	PEG	K_2CO_3	rt	6	75
17	1	5	PEG	K_2CO_3	rt	4	88

[a]Reaction conditions: PhI (1.0 mmol), Base (1.5 mmol)
[b]Isolated Yield.

The model reaction was carried out in the presence of different solvents, bases and different amounts of reactants and catalyst. The best results were obtained with PhI (1.0 mmol) and Ph_3SnCl (0.5 mmol) in the presence of MCM-41-dtz-Pd(II) (5 mg), K_2CO_3 (1.5 mmol) as base and PEG-400 as solvent at room temperature (Table 6, entry 3). After optimizing the reaction conditions, the C-C coupling reaction of various aryl halides with Ph_3SnCl were tested. Results have been summarized in Table 7.
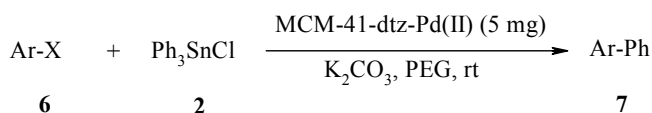
$$\text{Ar-X} \quad + \quad Ph_3SnCl \xrightarrow[\text{K_2CO_3, PEG, rt}]{\text{MCM-41-dtz-Pd(II) (5 mg)}} \text{Ar-Ph}$$
$$\textbf{6} \qquad\qquad \textbf{2} \qquad\qquad\qquad\qquad\qquad \textbf{7}$$

Table 7. Coupling reaction of aryl halides with Ph_3SnCl catalyzed by MCM-41-dtz-Pd(II) in PEG-400 at room temperature

Entry	ArX 6	Time (h)	Yield 7 (%)[a,b]	Mp (°C) [Ref.]
1	PhI	3	97	69 [38]
2	4-MeOPhI	4	80	87-89 [39]
3	4-MePhI	3.5	94	46-47 [40]
4	PhBr	3	95	69 [38]
5	4-MePhBr	3.3	85	46-47 [41]
6	2-MePhBr	5	78	Colorless oil [40]
7	4-NCPhBr	2	94	86-87 [38]
8	4-NO_2PhBr	2	92	112-114 [41]
9	PhCl	8	80	69 [38]
10	4-NO_2PhCl	5	90	112-114 [41]
11	1-NaPhI	6	90	44-46 [17]
12	1-NaPhBr	7	88	44-46 [17]

[a] All the products were identified and characterized by comparison of their physical and spectral data with those of authentic samples. [b] Isolated yield.

Finally, the reusability of the MCM-41-dtz-Pd(II) was investigated. Fig 7 shows the yield of five consecutive cycles for the preparation of 1,1'-biphenyl (a), diphenyl ether (b) and diphenyl amine (c). After the reaction reached the completion, the catalyst was recovered, washed with ethanol and water then reused in the next run. The catalyst has been observed to be reusable for at least five times without a detectable catalytic leaching or an appreciable change in activity (Fig. 7). High and reproducible catalytic activity and significantly low leaching of Pd (during catalytic reactions) from MCM-41 functionalised with dithizone (dtz) group was observed (about 3%), the amount of Pd in the five recovery determined by EDS spectrum

(based on EDS measurement W% of Pd has been determined for unreacted catalyst: 33.89%; after first run: 29.89% and after fifth run: 26.19%). Also, the nature of the recovered catalyst was investigated by IR (Fig. 1e).
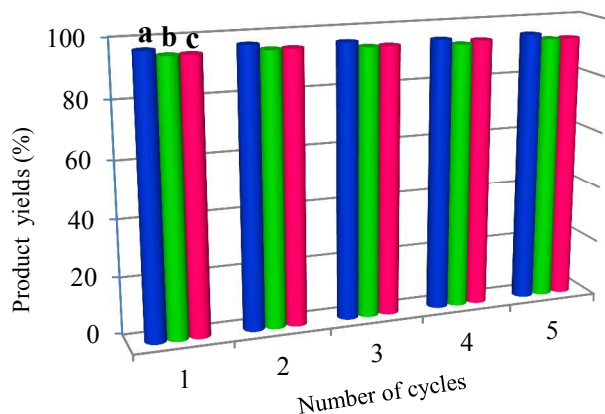

Figure 7. Reusability of MCM-41-dtz-Pd(II) in the Stille cross-coupling reaction (columns a), C-O bond formation (columns b) and C-N bond formation (columns c).

3 Conclusions

In conclusion, a novel mesoporous silica supported Pd(II) complex (MCM-41-dtz-Pd(II)) has been prepared through sequential grafting of several organic molecules. FT-IR, XRD, SEM, TGA, ICP-OES, EDS and BET surface area analysis studies suggested the functionalization of Pd(II) in the surface of the mesopores silica. MCM-41-dtz-Pd(II) has high thermal and chemical stability and is an efficient and recyclable catalyst for the coupling of a wide variety of aryl halides, phenols and amines with Ph_3SnCl. The ease of preparation, long shelf life, simple separation from the reaction mixture, stability toward air and compatibility with a wide variety of coupling reactions make it an ideal green heterogeneous catalyst. Moreover, the catalyst could be reused for several cycles without significant loss of stability and activity. These advantages make the process valuable from the synthetic and environmental points of view.

4 Experimental

4.1. Material and physical measurements

The cationic surfactant cetyltrimethylammonium bromide (CTAB, 98%), tetraethyl orthosilicate (TEOS, 98%), sodium hydroxide, aryl halide, triphenyltin chloride, phenols, amines and solvents were purchased from Merck and Aldrich and used without further purification. Catalyst was characterized by XRD patterns, which were collected on a Scintag PAD V X-Ray diffractometer using a Co radiation source with a wavelength $\lambda = 1.78897$ Å, 40 kV. The particle morphology was examined by measuring SEM using FESEM-TESCAN MIRA3, TEM analysis of the catalyst was recorded using a Zeiss-EM10C TEM. IR spectra were recorded as KBr pellets on a VRTEX 70 model BRUKER FT-IR spectrophotometer. NMR spectra were recorded on a Bruker AVANCE DPX-250 (250 MHz for ^{1}H). Chemical shifts are given in ppm (δ) relative to internal TMS and coupling constants J are reported in Hz. Mass spectra were recorded on an Agilent-5975C

inert XL MSD mass spectrometer operating at an ionization potential of 70 ev. Nitrogen adsorption isotherms were determined using a standard gas manifold at 77 K to characterize material properties such as catalyst surface area, pore volume, and average pore diameter. Moreover, adsorption data are presented in both the method of Brunauer and Emmet. Thermogravimetric analysis (TGA) was carried out on Shimadzu DTG-60 instrument. The content of Pd was measured by inductively coupled plasma-optical emission spectrometry (ICP-OES). Melting points were measured with an Electrothermal 9100 apparatus.

4.2 Preparation of mesoporous silica-anchored MCM-41-dtz-Pd(II)

Mesoporous Si-MCM-41 was synthesized according to the literature method [42]. To a mixture of NaOH (1.2 g) and cetyltrimethylammonium bromide (CTAB) (3.64 g), deionized water (108 mL) was added and followed by slowly and continuously adding tetraethyl orthosilicate (TEOS, 20.41 g). After 1 h stirring, the obtained synthetic solution with molar composition $1/0.1/0.3/60$ $TEOS/CTAB/NaOH/H_2O$ was poured into a teflon bottle and placed in the autoclave at $100°C$ for 96 h. After cooling to room temperature, the resulting solid was gathered by filtration, washed with deionized water and dried at 70 °C followed by calcination at $550°C$ for 5 h with rate of $2°C/min$. to remove the residual surfactants. This mesoporous material is designated as Si-MCM-41. Functionalization of MCM-41 was performed by refluxing 4.8 g of Si-MCM-41 with 5 g of 3-chloropropyltrimethoxysilane (CPTMS) in n-hexane (96 mL) under nitrogen atmosphere for 24 h. The resulting solid $MCM-41-(CH_2)_3-Cl$ was filtered and washed with n-hexane for several times and dried under vacuum. Then, $MCM-41-(CH_2)_3-Cl$ (3 g) and dithizone (7.0 mmol) were added to a 250 mL round-bottomed flask containing DMF (20 mL) equipped with a magnetic stirrer bar. The reaction mixture was stirred for 30 h at 100 °C, filtered, washed thoroughly with ethanol and dried in vacuum for 12 h. The dithizone-functionalized MCM-41 (MCM-41-dtz) (3.0 g) was treated with ethanol (50 mL) for 30 min. An ethanolic solution of $Pd(OAc)_2$ (1.2 g) was added and the resulting mixture was refluxed for 15 h. The resulting black solid impregnated with the metal complex was filtered and washed with ethanol to obtain MCM-41-dtz-Pd(II) .

4.3 General procedure for *O*-phenyltion of phenols and *N*-phenylation of amines with Ph_3SnCl catalyzed by MCM-41-dtz-Pd(II)

The prepared catalyst (5 mg) was added to a mixture of phenol or amine derivative (1.0 mmol), triphenyltin chloride (0.5 mmol) and triethylamine (10 eq., 1.4 mL) at room temperature. The progress of the reaction was monitored by TLC. The reaction mixture was stirred within 24 h for O-phenylation and 15 h for N-phenylation. The catalyst was then filtered, washed with acetonitrile and water, vacuum dried and stored for subsequent runs. The aqueous solution was extracted with ethyl acetate and dried over $MgSO_4$. After evaporation of the solvent under reduced pressure, the product was crystallized from ethanol to afford arylphenyl ether or N-phenyl amine. The products may be purified by column chromatography on silica gel using n-hexane/EtOAc (3/1) if needed. Reaction products were characterized by IR, ^{1}H NMR and MS spectra. Spectroscopy data for compounds **3** and **5** are in good agreement with those previously reported.

1-Methoxy-4-phenoxybenzene (Table 3, entry 4): Yellowish oil [32]. ^{1}H NMR (250 MHz, $CDCl_3$): δ (ppm) 3.80 (s, 3H), 6.68 (d, $J = 9.0$

Hz, 2H), 7.21-7.58 (m, 7H); EI-MS (70eV): m/z (%) = 200 (M$^+$, 100).

Diphenylamine (Table 5, entry 1): White crystals, mp. 54-55 ^{o}C [34]. ^{1}H NMR (250 MHz, CDCl$_3$): δ (ppm) 5.73 (s, br, 1H), 6.95 (t, J = 7.2Hz, 2H), 7.10 (d, J = 8.0Hz, 4H), 7.26-7.32 (m, 4H); EI-MS (70eV): m/z (%) = 169 (M$^+$, 100).

4-Nitro-*N*-phenylaniline (Table 5, entry 6): yellow solid, mp. 134-136 ^{o}C [35]. ^{1}H NMR (250 MHz, CDCl$_3$): δ (ppm) 6.50 (s, br, 1H), 6.94 (d, J = 9.0 Hz, 2H), 7.25-7.37 (m, 3H), 7.55 (t, J = 7.2 Hz, 2H), 8.19 (d, J = 9.0 Hz, 2H); EI-MS (70eV): m/z (%) = 214 (M$^+$, 100).

4.4 General procedure for Stille-coupling of aryl halides with Ph$_3$SnCl catalyzed by MCM-41-dtz-Pd(II)

Aryl halide (1.0 mmol) was added to a stirring mixture of catalyst (5 mg) in PEG-400. Then, Ph$_3$SnCl (0.5 mmol) and K$_2$CO$_3$ (1.5 mmol) were added and stirred at room temperature. Monitoring of the reaction with TLC analysis shown the reaction was completed within 3 h. After the completion of the reaction, the catalyst was separated by filtration and the reaction mixture was extracted with H$_2$O and EtOAc. The organic layer was dried over MgSO$_4$ and then evaporated under reduced pressure. The residue was purified by column chromatography on silica gel using *n*-hexane/EtOAc (7/3), afforded the desired products in good to excellent yields.Reaction products were characterized by IR, ^{1}H NMR and MS spectrometry. Spectroscopy data for compounds **7** are in good agreement with those previously reported.

Biphenyl (Table 7, entries 1, 4 and 9): White solid, mp. 69 ^{o}C [38]. ^{1}H NMR (250 MHz, CDCl$_3$): δ (ppm) 7.36-7.39 (m, 2H), 7.46-7.52 (m, 4H), 7.64 (d, J = 7.5Hz, 4H); EI-MS (70eV): m/z (%) = 154 (M$^+$, 100).

2-Methylbiphenyl (Table 7, entry 6): Colourless oil [40]. ^{1}H NMR (250 MHz, CDCl$_3$): δ (ppm) 2.46 (s, 3H), 7.25-7.57 (m, 9H); MS (EI$^+$): m/z: 168 (M$^+$, 100).

Acknowledgements

References

^{a} *Department of chemistry, Faculty of Science, Ilam university, P. O. Box69315516, Ilam, Iran. E-mail:* *arashghch58@yahoo.com or a.ghorbani@mail.ilam.ac.ir*
^{b} *Department of Chemistry, Faculty of Sciences, University of Kurdistan, P.O. Box 66315-416, Sanandaj, Iran.*
^{c} *Department of Environment, Faculty of Natural Resource, University of Kurdistan, Postal code: 66177-15177,Sanandaj, Iran.*

1. J. S. Beck, J. C. Vartuli, W. J. Roth, M. E. Leonowicz, C. T. Kresge, K. D. Schmitt, C. T. W. Chu, D. H. Olson, E. W. Sheppard, S. B. McCullen, J. B. Higgins, J. L. Schlenker, *J. Am. Chem. Soc.* 1992, **114**, 10834.

2. C. T. Kresge, M. E. Leonowicz, W. J. Roth, J. C. Vartuli, J. S. Beck, *Nature,* 1992, **359**, 710.

3. Y. Wu, Y. Zhang, J. Cheng, Z. Li, H. Wang, Q. Sun, B. Han, Y. Kong, *Micro Meso. Mater.* 2012, **162**, 51.

4. S. Han, W. Hou, Z. Li, *Colloid Polym. Sci.* 2004, **282**, 1286.

5. Y. Chen, X. Shi, B. Han, H. Qin, Z. Li, Y. Lu, J. Wang, Y. Kong, *J. Nanosci. Nanotech.* 2012, **12**, 7239.

6. F. Torney, B. G. Trewyn, V. S. Y. Lin, K. Wang, *Nature Nanotech.* 2007, **2**, 295.

7. M. Hajjami, F. Ghorbani, F. Bakhti, *Appl. Catal. A.* 2014, **470**, 303.

8. R. M. Martin-Aranda, J. Cejka, *Top Catal.* 2010, **53**,141.

9. L. Lv, K. Wang, X. S. Zhao, *J. Colloid Interface Sci.* 2007, **305**, 218.

10. M. Yoshikazu, Y. Masanori, A. Eiichi, A. Sadao, T. Shunsuke, *Ind. Eng. Chem. Res.* 2009, **48**, 938.

11. I. I. Slowing, J. L. Vivero-Escoto, C. W. Wu, V. S. Y. Lin, *Adv. Drug Deliv. Rev.* 2008, **60**, 1278.

12. J. Y. Ying, C. P. Mehnert, M. S. Wong, *Ang. Chem. Int. Ed.* 1999, **38**, 56.

13. J. Demel, Sujandi, S-E. Park, J. Cejka, P. Stepnicka, *J. Mol. Catal. A: Chem.* 2009, **302**, 28.

14. J. Demel, M. Lamac, J. Cejka, P. Stepnicka, *chem. Sus chem.* 2009, **2**, 442.

15. B. Karimi, S. Abedi, J. H. Clark , V. Budarin, *Angew.Chem., Int. Ed.* 2006, **45**, 4776.

16. M. Bakherad, A. Keivanloo, B. Bahramian, S. Jajarmi, *J. Organomet. Chem.* 2013, **724**, 206.

17. N. Iranpoor, H. Firouzabadi, E. EtemadiDavan, A. Rostami, A. Nematollahi, *J. Organomet. Chem.* 2013, **740**, 123.

18. H. J. Xu, Y. F. Liang, Z. Y. Cia, H. X. Qi, C. Y. Yang, Y. S. Feng, *J. Org. Chem.* 2011, **76**, 2296.

19. S. Varghese, C. Anand, D. Dhawale, A. Mano, V. V. Balasubramanian, G. Allen Gnana Raj, S. Nagarajan, M. A. Wahab, A. Vinu, *Tetrahedron Letters.* 2012, **53**, 5656

20. L. Zhong, A. Chokkalingama, W. S. Chaa, K. S. Lakhia, X. Su, G. Lawrence, A. Vinu, *Catalysis Today.* 2015, **243**, 195.

21. M. Semler, P. Stepnicka, *Catalysis Today.* 2015, **243**, 128.

22. K. Köhler, R. G. Heidenreich, J. Pietsch, *Chem. Eur. J.* 2002, **8**, 622.

23. D. E. Bergbreiter, P. L. Osburn, J. D. Frels, *J. Am. Chem. Soc.* 2001, **123**, 11105.

24. J. M. Zhou, R. X. Zhou, L. Y. Mo, S. F. Zhao, X. M. Zheng, *J. Mol. Catal.* 2002, **178**, 289.

25. M. Opanasenko, P. Stepnicka, J. Cejka, *RSC Adv.* 2014, **4**, 65137.

26. M. Nikoorazm, A. Ghorbani-Choghamarani, F. Ghorbani, H. Mahdavi, Z. Karamshahi, *J. Porous. Mater.* 2015, **22**, 261.

27. M. Abrantes, A. Sakthivela, C. C. Romão, F. E. Kühn, *J. Organomet. Chem.* 2006, **691**, 3137.

28. Y. D. Xia, W. X. Wang, R. Mokaya, *J. Am. Chem. Soc.* 2005, **127**, 790.

29. F. J. Brieler, P. Grundmann, M. Fröba, L. Chen, P. J. Klar, W. Heimbrodt, H. A. Krug von Nidda, T. Kurz, A. Loidl, *J. Am. Chem. Soc.* 2004, **126**, 797.

30. H. J. Cristau, P. P. Cellier, S. Hamada, J. F. Spindler, M. Taillefer, *Org. Lett.* 2004, **6**, 913.

31. A. B. Naidu, E. A. Jaseer, G. Sekar, *J. Org. Chem.* 2009, **74**, 3675.

32. D. Ma, Q. Cai, *Org. Lett.* 2003, **5**, 3799.

33. V. Avudoddi, V. K. G. Palle, V. R. Pallapothula, *Eur. J. Chem.* 2012, **3**, 298.

34. L. Rout, P. Saha, S. Jammi, T. Punniyamurthy, *Adv. Synth. Catal.* 2008, **350**, 395.

35. X. Zhu, L. Su, L. Huang, G. Chen, J. Wang, H.Song, Y. Wan, *Eur. J. Org. Chem.* 2009, **2009**, 635.

36. K. W. Anderson, M. Mendez-Perez, J. Priego, S. L. Buchwald, *J. Org. Chem.* 2003, **68**, 9563.

37. H. Xu, C. Wolf, *Chem. Commun.* 2009, 1715.

38. J. Yang, L. Wang, *Dalton Trans.* 2012, **41**, 12031.

39. M. Cao, Y. Wei, S. Gao, R. Cao, *Catal. Sci. Technol.* 2012, **2**, 156.

40. K. Tanimoro, M. Ueno, K. Takeda, M. Kirihata, S. Tanimori, *J. Org. Chem.* 2012, **77**, 7844.

41. P. R. Verma, S. Mandal, P. Gupta, B. Mukhopadhyay, *Tetrahedron Lett.* 2013, **54**, 4914.

42. H. Chen, Y. Wang, *Ceramics Int.* 2002, **28**, 541.